

Structural and Optical Properties of $\text{Cd}_{1-x}\text{Fe}_x\text{Se}$ Microstructures Grown by Metalorganic Chemical Vapor Deposition

Z. G. Ju,^{†,‡} Y. M. Lu,[†] J. Y. Zhang,^{*,†} X. J. Wu,^{†,‡} K. W. Liu,^{†,‡} C. X. Shan,[†] B. S. Li,[†] D. X. Zhao,[†] Z. Z. Zhang,[†] B. H. Li,[†] B. Yao,[†] and D. Z. Shen[†]

Key Laboratory of Excited State Processes, Changchun Institute of Optics, Fine Mechanics and Physics, Chinese Academy of Sciences, 16 East Nan-Hu Road, Open Economic Zone, Changchun 130033, People's Republic of China, and Graduate School of the Chinese Academy of Sciences, 100039, People's Republic of China

Received September 2, 2007; Revised Manuscript Received April 2, 2008

ABSTRACT: Diluted magnetic semiconductors $\text{Cd}_{1-x}\text{Fe}_x\text{Se}$ were grown by metalorganic chemical vapor deposition. Their structure was studied by X-ray diffraction and selected area electron diffraction. The effect of Fe doping on the morphology and photoluminescence of CdSe was investigated. The photoluminescence study indicated that the crystalline structure of the $\text{Cd}_{1-x}\text{Fe}_x\text{Se}$ films changed from a mixture of cubic and hexagonal phase to a single hexagonal phase with increasing Fe content.

1. Introduction

Considerable research efforts have been focused on the synthesis and optical properties of diluted magnetic semiconductors (DMS).¹ However, most of the efforts so far are on bulk DMS.² The understanding of the fundamental structure and optical properties in low-dimensional DMS is crucial to the development of magneto-optical devices based on microstructures. Mn based microstructures have been studied extensively.³ A natural development of DMS is the growth of microstructures containing other transitional metals, in particular, Fe^{2+} . Microstructures based on Fe are not a simple extension of the DMS family, because the physical situations in this case differs completely from those in Mn-based compounds thanks to the substitutional Fe^{2+} possessing both spin and orbital momenta ($S = 2$, $L = 2$). However, the growth method and optical properties of Fe-based DMS microstructures are seldom reported, especially for the alloy of CdSe and FeSe. As CdSe is used as a candidate material for light-emitting devices,⁴ detectors,⁵ and FeSe has a high curie temperature (above room temperature),⁶ it must be very exciting to investigate CdFeSe. However, up to now, no paper involving Fe-based DMS microstructure $\text{Cd}_{1-x}\text{Fe}_x\text{Se}$ can be found. The introducing of Fe^{2+} to CdSe microstructures will significantly affect the formation and properties of the latter. Nevertheless, it is not very clearly how the morphology, phase, and size of the microstructure will be affected by the Fe concentration. Thus it is necessary to clarify these questions for the fabrication of Fe-based DMS microstructures.

In this paper, $\text{Cd}_{1-x}\text{Fe}_x\text{Se}$ hexagonal multilayer microstructures were obtained without any catalysts by metalorganic chemical vapor deposition (MOCVD). The effect of Fe content on the structure, morphology, and crystalline phase of the $\text{Cd}_{1-x}\text{Fe}_x\text{Se}$ microstructures was studied.

2. Experimental Section

The $\text{Cd}_{1-x}\text{Fe}_x\text{Se}$ microstructures were deposited on Al_2O_3 (0001) substrate using a MOCVD system with horizontal rectangular quartz

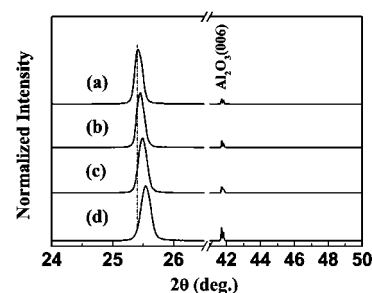


Figure 1. Normalized XRD diffraction patterns of $\text{Cd}_{1-x}\text{Fe}_x\text{Se}$ samples: $x =$ (a) 0.0, (b) 0.012, (c) 0.027, and (d) 0.035.

chamber. The growth temperature was 713 K and the pressure was 2×10^4 Pa. Dimethylcadmium (DMCd), ironpentacarbonyl ($\text{Fe}(\text{CO})_5$) and hydrogen selenide (H_2Se) were used as precursors. Ultrahigh purity hydrogen was used as carrier gas. The substrates were cleaned by soaking in acetone and ethanol for 5 min in an ultrasonic bath and etched in an acid solution ($3\text{H}_2\text{SO}_4 + 1\text{H}_3\text{PO}_4$) for 5 min at 433 K, followed by a deionized water rinse. Then the substrates were loaded into the MOCVD chamber and heated to 873 K in H_2 ambient. During deposition, the DMCd precursor was transported into the chamber at a flow rate of 8 mL/min, and H_2Se at 15 mL/min. The flow rate of $\text{Fe}(\text{CO})_5$ was varied to obtain $\text{Cd}_{1-x}\text{Fe}_x\text{Se}$ with different Fe content. In our experiment, four samples with $x = 0, 0.012, 0.027,$ and 0.035 were prepared.

The structure of samples was characterized by X-ray diffraction (XRD) with $\text{Cu K}\alpha$ radiation ($\lambda = 0.154178$ nm) with $\theta-2\theta$ (Bragg-Brentano) configuration (Ringaku O/max-RA). The general morphology was examined using a scanning electron microscope (SEM) with operating voltage of 20 KeV (HITACHI, S-4800). The thickness of the samples was about 500 nm measured from the cross-sectional SEM images. The composition was determined by an energy dispersive X-ray spectrometer (EDS) (GENESIS 200 XMS 60S) attached to the SEM. The structure of single sheet was examined by selected area electron diffraction (SAED). Photoluminescence (PL) spectra of the samples were measured by 488 nm laser with a liquid nitrogen cooled cryostat (TMS 94).

3. Results and Discussion

Figure 1 shows the XRD patterns of the $\text{Cd}_{1-x}\text{Fe}_x\text{Se}$ samples grown on sapphire substrate with different Fe content. For as-grown CdSe sample, besides the diffraction peak at 41.68° from the sapphire substrate, only one diffraction peak located at about 25.40° is observed. CdSe can exist in zinc-blende or wurtzite

* Corresponding author. Tel: 86 43186176322. Fax: 86 43185682964. E-mail: zhangjy53@yahoo.com.cn.

[†] Changchun Institute of Optics, Fine Mechanics and Physics, Chinese Academy of Sciences.

[‡] Graduate School of the Chinese Academy of Sciences.

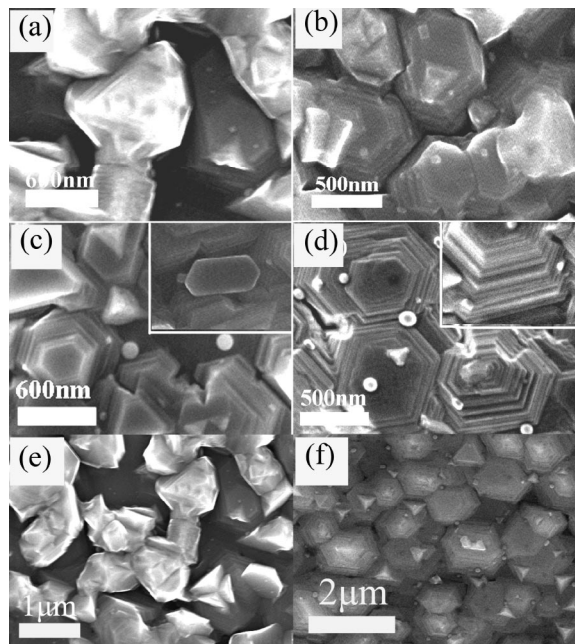


Figure 2. Plan-view SEM images of $\text{Cd}_{1-x}\text{Fe}_x\text{Se}$ samples for $x =$ (a) 0.0, (b) 0.012, (c) 0.027, (d, f) 0.035.

structure.⁷ Because the zinc-blende (111) overlaps with the wurtzite (002) peak, it is hardly distinguishable by our XRD equipment for their very small position difference.⁸ Therefore, we cannot determine the crystalline structure only by XRD method. As seen in Figure 1, it is clear that the diffraction peak positions of the samples shifts to a larger angle with increasing Fe content. This phenomenon is usually attributed to the change in lattice spacing caused by the Fe incorporation. The gradually shrinking of the lattice spacing with increasing Fe content may reveal that Fe atoms enter the lattice sites in place of Cd atoms, because their atomic radii are 0.074 nm for Fe^{2+} and 0.097 nm for Cd^{2+} .

The plan-view SEM images of the as-prepared CdFeSe are shown in Figure 2, in which some irregular blocks are seen in Figure 2a. Figure 2b–d shows the morphologies of the samples with different Fe concentration. For the sample with 1.2% Fe content, steps appear on the edge of the blocks. When the Fe concentration is increased to 2.7%, most of the irregular blocks change into multilayer structures, as shown in Figure 2c. These multilayer structures cover most of the sample surface. Some of them are isolated, as illustrated in the inset of Figure 2c. The sizes of the hexagonal sheets are about 200–500 nm in diameter, and several nanometers in thickness. SAED shows that these sheets are single crystal, as illustrated in Figure 3d. When the Fe content is increased to 3.5%, hexagonal multilayer structures are well-formed, as shown in Figure 2d, whereas the surface blocks are nearly absent. The inset in Figure 2d shows an image of a hexagonal multilayer structure taken with the sample tilted by 30° with respect to the electron beam. The image shows that the hexagonal multilayer is built layer by layer, the diameter of the base is about 600 nm and that of the top is about 200 nm. The multilayers are almost vertical to the substrate. In Figure 2a–d, some nanoparticles are also observed on the sample surface, and they grow bigger and bigger with increasing Fe content. However, the attempt to find any relationship between the nanoparticles and the multilayers fails. Images a and b in Figure 3 are higher-magnification images of the nanoparticle and multilayer in sample $\text{Cd}_{0.965}\text{Fe}_{0.035}\text{Se}$, the EDS spectra of which is shown in Figure 3c. The EDS data

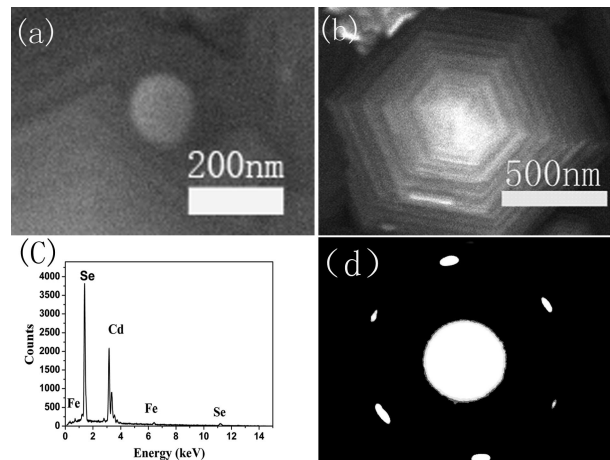


Figure 3. (a) SEM images of nanoparticles and (b) hexagonal microstructures in $\text{Cd}_{0.973}\text{Fe}_{0.027}\text{Se}$ sample, (c) EDS spectra, and (d) SAED pattern of a single sheet.

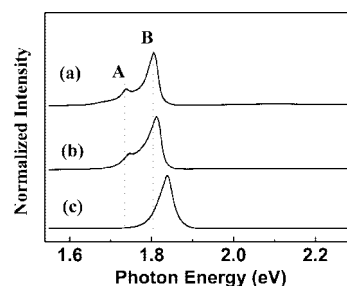


Figure 4. Normalized 82 K PL spectra of (a) CdSe , (b) $\text{Cd}_{0.988}\text{Fe}_{0.012}\text{Se}$, and (c) $\text{Cd}_{0.973}\text{Fe}_{0.027}\text{Se}$.

indicate that the Fe content ($x = 0.035$) in the two structures are the same. Images e and f in Figure 2 show the images of CdSe and $\text{Cd}_{0.965}\text{Fe}_{0.035}\text{Se}$; the two figures exhibit that the irregular blocks have been changed into regular hexagonal multilayers because of the introduction of Fe. From the above description, the conclusion that Fe has a positive effect on forming CdFeSe hexagonal multilayer structure can be drawn.

Figure 4a–c shows the PL spectra of $\text{Cd}_{1-x}\text{Fe}_x\text{Se}$ with different Fe content measured at 82 K. To observe the exactly position of the emission peak, the PL spectra have been normalized in height. As can be seen from Figure 4a, CdSe show two emission peaks with the energy difference of 66 meV, and they are labeled as A and B. The emission peak at higher energy is attributed to the band gap emission from the hexagonal phased CdSe , while the lower energy one from cubic CdSe . It is difficult to differentiate the mixed-phase structure from the XRD patterns because of the fact that in CdSe , three strongest zinc-blende peaks (111), (220), and (311) overlap correspondingly with 002, 110, and 112 peaks of wurtzite. However, the PL can distinguish the two phases due to the large difference (~ 100 meV) in the band gap of cubic and hexagonal-phased CdSe .⁸ Moreover, the XRD patterns can hardly detect the impurity phase when the component of the impurity is less than 5%, whereas the PL spectra measured by micro area can. That means PL spectra can be an indirectly but effective way to determine the crystalline structure and detect the impurity phase in CdSe .⁹ As shown in Figure 4, both peaks show a blue shift with increasing Fe content, which can be understood by considering that FeSe has a wider band gap (3.0 eV) than CdSe .¹³ Moreover, the relative intensity of peak A to B becomes smaller and smaller with increasing Fe content, and peak A

almost disappears when the Fe content reaches 2.7%, as shown in Figure 4c, which indicates that the structure of the samples changes from mixed phase (for samples CdSe and Cd_{0.988}Fe_{0.012}Se) to pure hexagonal phase (for samples Cd_{0.973}Fe_{0.027}Se and Cd_{0.965}Fe_{0.035}Se) caused by the incorporation of Fe²⁺. CdSe prefers to crystallize in wurtzite and cubic mixed phase under present experiment conditions.¹⁰ When Fe²⁺ is introduced into the lattice of zinc blende CdSe, the metastable cubic structure will tend to crystallize in stable wurtzite phase for FeSe forms hexagonal phase under the employed growth conditions.¹¹ The above facts suggest that the introducing of Fe into CdSe lattice can increase the relative stability of wurtzite phase of CdSe, which is similar to the results reported in the ZnMgO system.¹²

The formation of CdFeSe multilayers may originate from two-dimensional layer-by-layer growth processes in MOCVD system. The growth undergoes a three-dimensional mode before introducing Fe, as seen in Figure 2a. After Fe is introduced to the system, the growth mode is changed to a quasi-two-dimensional layer-by-layer process, as shown in Figure 2d. However, the nucleated rate of new CdFeSe grains is larger than the growth rate of the prelayers, which means the new layer will begin to grow before the prelayer has grown up. This is so-called kinetic confinement, which will result in the steps on the side surface of CdFeSe. The same growth principle has been reported in ZnO nanotower growth process.¹³ More Fe doping will help to form hexagonal multilayer and large nanoparticles. Hence, Fe doping has positive effect on the formation of Cd_{1-x}Fe_xSe microstructures; it can modify the sample surface and stabilize the wurtzite phase of CdFeSe. Moreover, the size of the microstructure can be tuned by changing the Fe concentration.

4. Conclusion

In summary, Cd_{1-x}Fe_xSe multilayer structures have been realized by MOCVD without any catalysts. XRD, SEM, SAED,

and PL prove that Fe doping can modify the sample surface, improve the optical quality of samples, and conduce to the formation of microstructure. Moreover, the introduction of Fe²⁺ is helpful for CdSe to form stable wurtzite structure.

Acknowledgment. This work is supported by the Key Project of National Natural Science Foundation of China under Grant 60336020 and 50532050, the "973" program under Grant 2006CB604906, the Innovation Project of Chinese Academy of Sciences, and the National Natural Science Foundation of China under Grant 60429403, 60506014, and 10674133.

References

- (1) Liu, X.; Petrou, A.; Jonker, B. T.; Prinz, G. A.; Krebs, J. J.; Warnock, J. *Appl. Phys. Lett.* **1988**, *53*, 476.
- (2) Stankiewicz, J.; Lorenzo, M. D. *J. Appl. Phys.* **1991**, *69*, 1479.
- (3) Liu, J. J.; Yu, M. H.; Zhou, W. L. *J. Appl. Phys.* **2006**, *99*, 08M119.
- (4) Matsumura, N.; Endo, H.; Saraie, J. *Phys. Status Solidi B* **2002**, *229*, 1039.
- (5) Hernandez, C. F.; Suh, D. J.; Kippelen, B.; Marder, S. R. *Appl. Phys. Lett.* **2004**, *85*, 534.
- (6) Feng, Q. J.; Shen, D. Z.; Zhang, J. Y.; Li, B. S.; Li, B. H.; Lu, Y. M.; Fan, X. W.; Liang, H. W. *Appl. Phys. Lett.* **2006**, *88*, 012505.
- (7) Ninomiya, S.; Adachi, S. *J. Appl. Phys.* **1995**, *78*, 4681.
- (8) Shan, C. X.; Liu, Z.; Ng, C. M.; Hark, S. K. *Appl. Phys. Lett.* **2005**, *86*, 213106.
- (9) Ju, Z. G.; Lu, Y. M.; Shan, C. X.; Zhang, J. Y.; Yao, B.; Shen, D. Z. *J. Phys. D: Appl. Phys.* **2008**, *41*, 015304.
- (10) Ju, Z. G.; Lu, Y. M.; Zhang, J. Y.; Wu, X. J.; Liu, K. W.; Zhao, D. X.; Zhang, Z. Z.; Li, B. H.; Yao, B.; Shen, D. Z. *J. Cryst. Growth* **2007**, *307*, 26.
- (11) Wu, X. J.; Zhang, Z. Z.; Zhang, J. Y.; Li, B. H.; Ju, Z. G.; Lu, Y. M.; Li, B. S.; Shen, D. Z. *J. Appl. Phys.* **2008**, submitted.
- (12) Chen, N. B.; Wu, H. Z.; Qiu, D. J.; Xu, T. N.; Chen, J.; Shen, W. Z. *J. Phys: Condens. Matter* **2004**, *16*, 2973.
- (13) Tong, Y. H.; Liu, Y. C.; Shao, C. L.; Wu, R. X. *Appl. Phys. Lett.* **2006**, *88*, 123111.

CG700837U